IJSES
Volume 9, Issue 7, pp. 36-45, 2025.
International Journal of Scientific Engineering and Science
ISSN (Online): 2456-7361

Spatial Distribution of Natural Radioactivity from the ^{238}U and ^{232}Th Decay Series, and ^{40}K in the Volcanic Soils of Nosy-Be Island, Madagascar

DJAOVAGNONO Houssen Claude[1], DONNE Zafizara[1], RASOLONIRINA Martin[2], SOLONJARA Asivelo Fanantenansoa[2], KALL Briant[1]
[1]Department of Nuclear Metrology and Environment, Faculty of Science, University of Antsiranana, Madagascar
[2]Department of Nuclear Techniques and Analysis, National Institute of Sciences and Nuclear Techniques, Madagascar

***Abstract*—*This study presents the first comprehensive characterization of natural radioactivity in the volcanic soils of Nosy-Be Island, Madagascar. The main objective was to quantify and map the spatial distribution of the specific activities of radionuclides from the ^{238}U and ^{232}Th decay series, as well as ^{40}K. A total of 30 soil samples, representative of the island's geo-pedological variability, were analyzed using gamma-ray spectrometry with a NaI(Tl) detector. The results indicate mean specific activities of 33 ± 8 Bq/kg for ^{238}U (2.66 ± 0.69 ppm), 39 ± 9 Bq/kg for ^{232}Th (9.53 ± 2.25 ppm), and 138 ± 79 Bq/kg for ^{40}K (0.44 ± 0.25%). These values position Nosy-Be as a region of moderate natural radioactivity, both in comparison to global averages and within the national context of Madagascar. The key contribution of this work lies in the identification of pronounced spatial heterogeneity, strongly driven by the island's geological and pedological duality. A clear contrast emerges between the western region, formed by recent Pleistocene volcanism, which exhibits elevated radionuclide concentrations and contains the identified hotspots, and the eastern region, dominated by older formations and deeply weathered ferrallitic soils, significantly depleted particularly in ^{40}K due to intense leaching processes. This study provides the first baseline radiological map of Nosy-Be, offering a critical foundation for future environmental assessments and for the sustainable management of the island's natural resources.*

***Keywords*—*Natural Radioactivity, Gamma-ray Spectrometry, Volcanic Soils, Spatial Distribution, Nosy-Be, Madagascar.*

I. INTRODUCTION

Natural radioactivity is a fundamental component of the Earth's environment. Human exposure to ionizing radiation, particularly gamma radiation originates largely from terrestrial sources, primarily the decay of primordial radionuclides. Among these, the decay chains of uranium-238 (^{238}U) and thorium-232 (^{232}Th), along with potassium-40 (^{40}K), are the dominant contributors [1-5]. However, the distribution of these radionuclides in soils and rocks is highly heterogeneous, being intrinsically controlled by local geological settings and environmental processes [1-3, 5-7].

This spatial heterogeneity stems from the distinct geochemical behaviors of these three naturally occurring radionuclides. As lithophile and incompatible elements, uranium, thorium, and potassium preferentially concentrate in the melt during magmatic differentiation, resulting in their natural enrichment in evolved igneous rocks such as granites and rhyolites. At the Earth's surface, however, their mobility diverges markedly due to weathering processes. Potassium, an alkali metal, is highly mobile; it is readily released from host minerals such as feldspars during chemical weathering, making it particularly prone to leaching under humid climatic conditions. Thorium, in contrast, is extremely immobile, it has very low solubility and is typically retained in situ within weathering profiles or mechanically concentrated in resistant heavy minerals. Uranium exhibits intermediate and highly variable mobility, strongly influenced by redox conditions: it may either remain immobilized in reducing environments or become soluble and transported under oxidizing conditions [8].

Understanding these geochemical distinctions is essential for interpreting radiological landscapes and explains why igneous and volcanic rocks often exhibit higher radionuclide concentrations than sedimentary formations, except for specific deposits such as clays, organic-rich shales, or heavy mineral sands [1, 2, 6, 9].

Mapping the spatial distribution of natural radionuclides is therefore crucial for environmental monitoring, health risk assessment, and sustainable land-use planning [4, 5, 9-11].

In this context, Nosy-Be, located off the northwest coast of Madagascar, presents a particularly compelling case study.

The island's complex Cenozoic volcanic history has resulted in a diverse geological mosaic of basalts, rhyolites, and syenites, giving rise to varied soil types [12-14]. Volcanic terrains are known to host elevated levels of natural radionuclides due to magmatic enrichment processes [15]. Moreover, Nosy-Be displays a pronounced geo-pedological duality: its western region is dominated by relatively recent volcanic rocks (Pleistocene) with young, weakly developed soils, while the eastern region features older geological formations overlaid by deeply weathered and intensely leached ferrallitic soils under a humid tropical climate [12-13]. This contrast strongly suggests differential radionuclide redistribution, governed by their respective mobilities in the weathering environment.

Despite its distinctive geological features and socio-economic importance, no scientific study has yet investigated the natural radioactivity of Nosy-Be. This lack of data hinders a proper assessment of baseline radiological conditions and limits our understanding of the geochemical processes driving radionuclide behavior in tropical volcanic settings.

International Journal of Scientific Engineering and Science
Volume 9, Issue 7, pp. 36-45, 2025. ISSN (Online): 2456-7361

This study aims to address this gap by providing the first quantitative characterization and spatial mapping of the specific activities of ^{238}U and ^{232}Th series radionuclides, as well as ^{40}K, in the soils of Nosy-Be Island. More specifically, it seeks to elucidate the relationship between the radiological signature of the soils and the island's contrasting geo-pedological units. The outcome is a baseline radiological map that will serve as a critical reference for future environmental assessments, radiological risk evaluations, and the sustainable management of the region.

II. Material and Methods

2.1. Study Area Description

The study was conducted on the Nosy-Be Island, which covers approximately 320 km^2 and is located off the northwest coast of Madagascar, in the DIANA region. The island lies between latitudes 13°09′45.13"–13°30′17.93" S and longitudes 48°07′31.92"–48°24′21.18" E (Fig. 1).

Nosy-Be exhibits a unique geo-climatic context. Its geology is characterized by a mosaic of Cenozoic volcanic formations overlying a Mesozoic sedimentary basement (Fig. 2). The area is subject to a humid tropical climate, with annual rainfall around 2200 mm and an average temperature of 25°C. These climatic conditions promote intense chemical weathering of parent materials, directly influencing soil formation and composition [12-14].

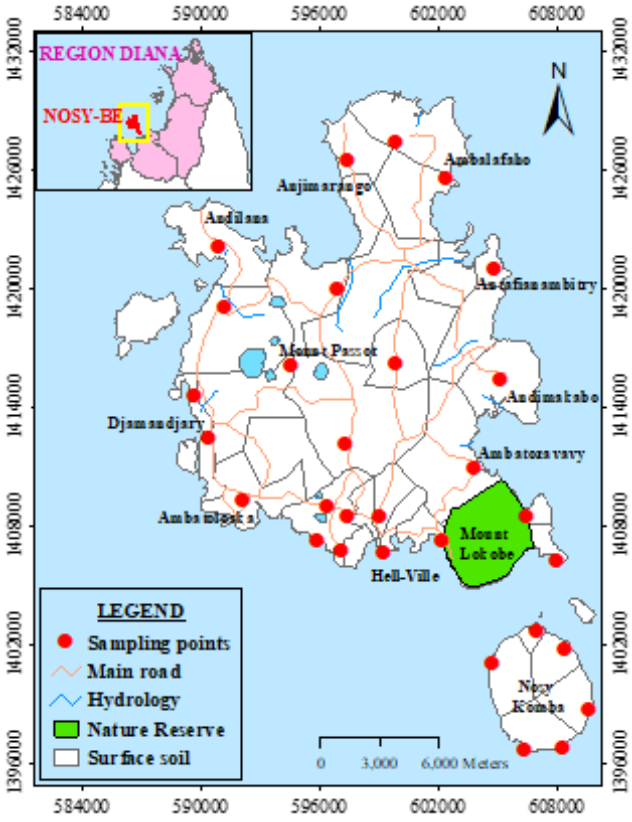

Fig. 1. Location of sampling points

The geological chronology of the island starts with a Mesozoic (Jurassic) sedimentary basement composed of marly and oolitic limestones, bituminous sandstones, argillites, and lignites, although these formations are now only sparsely exposed (Fig. 2). During the Cenozoic, this basement was intruded by plutonic rocks (granites, gabbros, and nepheline syenites) forming the Lokobe massif in the southeast. This was followed by an early volcanic phase (Neogene to Quaternary) that produced extensive basaltic and ankaratrite flows, particularly in the eastern and central regions. A more recent volcanic episode (Pleistocene) affected the western part of the island, creating features such as Mount Passot with rhyolitic, basaltic, and better-preserved ankaratrite flows. The most recent deposits (Holocene) consist of alluvium in valleys, mangrove muds in estuaries, and coastal dunes [12, 13]. This lithological diversity, coupled with strong weathering processes, results in a wide range of soils that significantly affect radionuclide distribution and behaviour [16, 17].

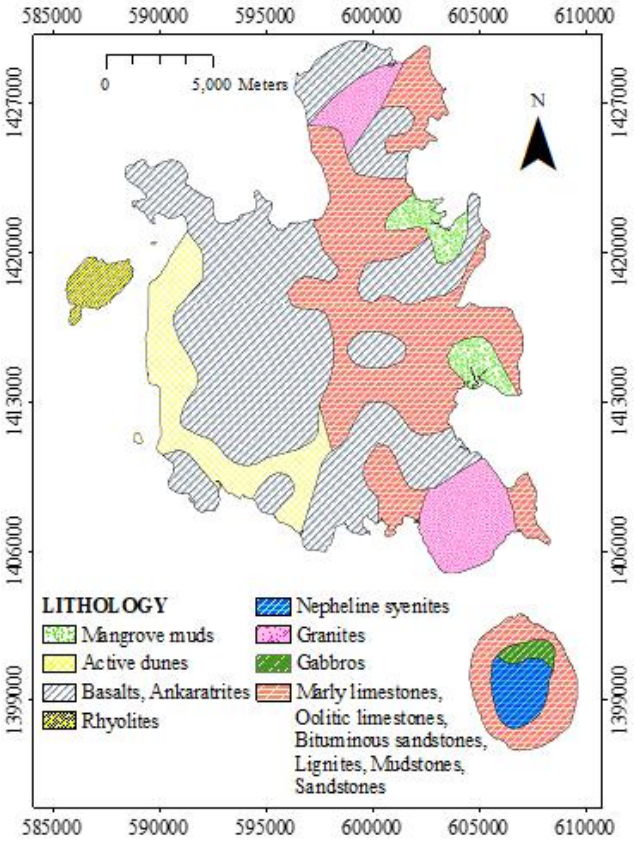

Fig. 2. General geological map of Nosy-Be, revised by Henri Besairie (1970)

Four main soil types are identified [12, 13]:

- Ferrallitic soils, developed over older formations (ancient basalts, granites), in the east and southeast, are deeply weathered, acidic (pH < 5.5), and highly leached. While potassium, a mobile element, is expected to be depleted, residual enrichment in less mobile elements like uranium and thorium may occur.
- Eutrophic brown soils, formed over recent volcanic materials (e.g., tuffs, ashes) in the west, are weakly developed but fertile, with near neutral pH. These soils may retain high levels of ^{40}K and potentially ^{238}U and ^{232}Th with unweathered primary minerals.
- Young poorly developed soils, found on recent deposits (e.g., valley alluvium and coastal sands), exhibit highly

variable chemical compositions that reflect the characteristics of upstream rocks.

- Hydromorphic soils, found in poorly drained areas (e.g., marshes, footslopes), are subject to reducing conditions due to water saturation. These conditions can increase the mobility of uranium and thus influence its distribution.

2.2. Sampling Strategy and Sample Preparation

Two field campaigns were conducted in August 2023 and May 2024. A total of 30 soil samples was collected to represent the geo-pedological variability of Nosy-Be. Sampling locations were selected based on geological diversity, land use (agriculture, forest, coastal, urban), and human activity levels, including areas frequently visited by the local population and tourists.

Each sampling point was geo-referenced using a GPS, and a map was generated with ArcGIS 10.5, using FTM (Foiben-Taosarintanin'i Madagasikara) base data and the Laborde coordinate system (Fig. 1).

At each site, approximately 300 g of soil was sampled from a 30 cm depth, after removing surface litter and debris to access undisturbed soil. Samples were stored in labelled plastic bags and coded from NB01 to NB30, with "NB" denoting Nosy-Be.

Following established procedures, samples were prepared in the laboratory at the Institut National des Sciences et Techniques Nucléaires (INSTN-Madagascar). Soil was oven-dried at 105°C, ground, and sieved to < 2 mm to obtain a fine, homogeneous powder. This powder was then sealed in 100 cm^3 polyethylene containers and stored for over three weeks to allow for secular equilibrium in the ^{238}U decay chain, particularly between ^{226}Ra and its progenies.

2.3. Gamma-ray Spectrometry Measurement

Quantitative analysis of the specific activities of ^{238}U, ^{232}Th, and ^{40}K was performed by gamma-ray spectrometry. The using the following setup [3, 10, 18]:

- Detector: A NaI(Tl) scintillation detector (ORTEC 905/4), 76.2 mm x 76.2 mm, coupled with a 14-stage dynode PMT;
- Electronics: A acquisition system (ORTEC digiBase) including preamplifier, amplifier, ADC, and MCA.
- Software: ScintiVision for spectrum acquisition and analysis;
- Shielding: A cylindrical shielding system consisting of 10 mm stainless steel and 30 mm lead to reduce background radiation.

The detector's full width at half maximum (FWHM) was 7.5% at 1332.5 keV (^{60}Co peak) [3, 10, 18].

Energy and efficiency calibrations were performed prior to measurements. The ambient background was measured using an empty 100 cm^3 container under identical conditions. Each sample was counted for 12 hours.

Energy calibration established a linear correlation between MCA channels and gamma energy.

Efficiency calibration followed the spectrum stripping method described by Rybach (1988) and Chiozzi et al. (2000) [10, 18-22], defining three energy windows (Fig. 3):

- K-window: ^{40}K, centered at 1461 keV;
- U-window: ^{214}Bi (from ^{238}U series), 1764.5 keV;
- Th-window: ^{208}Tl (from ^{232}Th series), 2614.5 keV.

Each window was widened to 15% of the peak energy, exceeding the 10% typically used, to integrate the full photopeak area.

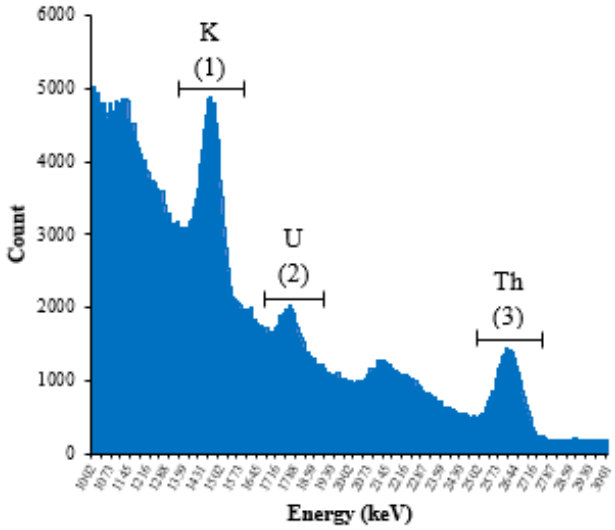

Fig. 3. Energy windows used to quantify ^{40}K, ^{238}U, and ^{232}Th

Table I summarizes the overlap in these windows, which was corrected using certified reference materials from the IAEA:

- RGK-1: High purity K_2SO_4, 448,000 ± 3000 µg/g; activity exclusively from ^{40}K;
- RGU-1: Uranium ore diluted with silica, 400 ± 2 µg/g of ^{238}U;
- RGTh-1: Thorium ore diluted with silica, 800 ± 16 µg/g of ^{232}Th.

Each standard was used to calculate stripping coefficients and efficiency constants per region of interest. The system of equations derived from these calibrations led to the creation of an efficiency matrix, which relates observed count rates to actual radionuclide activities.

TABLE I. Typical energy windows in gamma-ray spectrometry

ROI	Peak Energy [Radionuclide]	Energy ranges (keV)	Convolution*
(1)	1461 keV [^{40}K]	1351.4 – 1570.6	1377.7 (3.92; ^{214}Bi) 1401.5 (1.55; ^{214}Bi) 1407.9 (2.8; ^{214}Bi) 1461.0 (10.67; ^{40}K) 1509.2 (2.12; ^{214}Bi)
(2)	1764.5 keV [^{238}U series]	1632.2 – 1896.8	1661.3 (1.14; ^{214}Bi) 1666.5 (8.87; ^{228}Ac) 1729.6 (2.88; ^{214}Bi) 1764.5 (15.36; ^{214}Bi) 1847.4 (2.04; ^{214}Bi)
(3)	2614.5 keV [^{232}Th series]	2418.4 – 2810.6	2447.86 (1.50; ^{214}Bi) 2614.5 (99.16; ^{208}Tl)

* Energy (Intensity [%]; Element); ROI: Region of Interest

2.4. Determination of efficiency constants

The net count rate $R_{i,j}$ observed in a region of interest i for a given standard source j, depends on the activities $A_{n,j}$ of each

International Journal of Scientific Engineering and Science
Volume 9, Issue 7, pp. 36-45, 2025. ISSN (Online): 2456-7361

radionuclide n present in the standard. This relationship is expressed by the following equation [19,20, 22]:

$$R_{i,j} = \sum_{n=1}^{3} \varepsilon_{i,n} \times A_{n,j} \quad (1)$$

Where the indices i, j, and n (ranging from 1 to 3) respectively denote the regions of interest (1: K, 2: U, 3: Th), identifies the standard source (RGK-1, RGU-1, and RGTh-1), and corresponds to the radionuclide (^{40}K, ^{238}U, ^{232}Th). $\varepsilon_{i,n}$ is the detection efficiency for radionuclide n in ROI i. The net count rate is calculated using the following equation:

$$R_{i,j} = \frac{N_{i,j}}{t_j} - B_i \quad (2)$$

Where $N_{i,j}$ is the number of recorded counts in in ROI i for the standard j; t_j is the counting time for standard j; and B_i is the background count rate in ROI i.

Using Equation (1), an efficiency matrix (E) can be constructed, relating the net count rates in each ROI to the actual activities of the radionuclides in the standards.

For the RGK-1 standard, which primarily contains potassium, only the activity of ^{40}K is significant. The efficiency constant $\varepsilon_{1,1}$ representing the detection efficiency of ^{40}K in the K window, is calculated as:

$$\varepsilon_{1,1} = \frac{R_{1,1}}{A_{1,1}} \quad (3)$$

For the RGU-1 standard, the efficiency constants $\varepsilon_{1,2}$ and $\varepsilon_{2,2}$ were quantified using Equation (4):

$$\varepsilon_{1,2} = \frac{R_{1,2}}{A_{2,2}} \text{ and } \varepsilon_{2,2} = \frac{R_{2,2}}{A_{2,2}} \quad (4)$$

For the RGTh-1 standard, Equations (5) and (6) were used to determine the efficiency constants $\varepsilon_{1,3}$, and $\varepsilon_{2,3}$:

$$\varepsilon_{1,3} = \frac{1}{A_{3,3}}\left(R_{1,3} - \frac{A_{2,3}}{A_{2,2}} R_{1,2}\right) \quad (5)$$

$$\varepsilon_{2,3} = \frac{1}{A_{3,3}}\left(R_{2,3} - \frac{A_{2,3}}{A_{2,2}} R_{2,2}\right) \quad (6)$$

The constants $\varepsilon_{3,2}$ and $\varepsilon_{3,3}$ are determined by combining the uranium and thorium count rates in the third region of interest, as follows:

$$\varepsilon_{3,2} = \frac{R_{3,2}}{A_{2,2}} \text{ and } \varepsilon_{3,3} = \frac{1}{A_{3,3}}\left(R_{3,3} - \frac{A_{2,3}}{A_{2,2}} R_{3,2}\right) \quad (7)$$

2.5. Calculation of Radionuclide Specific Activities

The net count rates (R) for each region of interest are linked to radionuclide activities (A) via the matrix equation:

$$R = E \,.\, A \quad (8)$$

Where R is the vector of net count rates (R_K , R_U , R_{Th}) ; E is the efficiency matrix (3 x 3) determined during calibration, and A is the vector of unknown activities (A_K , A_U , A_{Th}). This can be written as [19, 20, 22]:

$$\begin{pmatrix} R_K \\ R_U \\ R_{Th} \end{pmatrix} = \begin{pmatrix} \varepsilon_{1,1} & \varepsilon_{1,2} & \varepsilon_{1,3} \\ 0 & \varepsilon_{2,2} & \varepsilon_{2,3} \\ 0 & \varepsilon_{3,2} & \varepsilon_{3,3} \end{pmatrix} \begin{pmatrix} A_K \\ A_U \\ A_{Th} \end{pmatrix} \quad (9)$$

To determine A, the equation is inverted:

$$\begin{pmatrix} A_K \\ A_U \\ A_{Th} \end{pmatrix} = \begin{pmatrix} a_{1,1} & a_{1,2} & a_{1,3} \\ 0 & a_{2,2} & a_{2,3} \\ 0 & a_{3,2} & a_{3,3} \end{pmatrix} \begin{pmatrix} R_K \\ R_U \\ R_{Th} \end{pmatrix} \quad (10)$$

This results in the following system of equations, where the coefficients $a_{i,j}$ are the elements of E^{-1}, the inverse of matrix E [19, 20, 22]:

$$\begin{cases} A_K = a_{1,1}R_K + a_{1,2}R_U + a_{1,3}R_{Th} \\ A_U = a_{2,2}R_U + a_{2,3}R_{Th} \\ A_{Th} = a_{3,2}R_U + a_{3,3}R_{Th} \end{cases} \quad (11)$$

Knowing that the constants of the inverse matrix E^{-1} must be expressed in terms of the efficiency constants $\varepsilon_{i,n}$ in the three regions of interest.

Uncertainties in activity were computed using by the law of error propagation. The overall uncertainty for each activity is given by [19, 20, 22]:

$$\sigma_{A_n} = \sqrt{\sum_i \left[\left(R_i \times \sigma_{a_{n,i}}\right)^2 + \left(a_{n,i} \times \sigma_{R_i}\right)^2\right]} \quad (12)$$

Where σ_{A_n} is the final uncertainty on the calculated activity for radionuclide n ; n is the index for the radionuclide whose activity is being calculated (n = 1 for ^{40}K, n = 2 for ^{238}U, and n = 3 for ^{232}Th) ; i is the index for each measurement window (i = 1 for the K window, i = 2 for the U window, and i = 3 for the Th window); $\sum_i$ is the summation over all measurement windows i ; $a_{n,i}$ is the coefficient of the inverse matrix that relates activity n to count rate i ; R_i is the net count rate in measurement window i ; $\sigma_{a_{n,i}}$ is the uncertainty on the matrix coefficient $a_{n,i}$; σ_{R_i} is the statistical uncertainty on the net count rate R_i .

The detection limit L_n was calculated using the Currie formula [18, 19]:

$$L_n = \frac{2\sqrt{2}}{\varepsilon_{i,n}} \times \sqrt{\left(\frac{B_i}{t}\right)} \quad (13)$$

Where B_i is the background count, $\varepsilon_{i,n}$ the efficiency, and t the counting time.

To facilitate interpretation, specific activities (in Bq/kg) were converted into elemental concentrations (in ppm or %) using [2, 24-27]:

$$E_C = \frac{A_E \times M_E \times C}{\lambda_E \times N_A \times f_{A,E}} \quad (14)$$

Where E_C represents the elemental concentration of the radionuclide E in the sample. The terms M_E, λ_E, $f_{A,E}$, and A_E respectively denote the atomic mass (kg/mol), the decay constant (s^{-1}), the natural isotopic abundance, and the measured specific activity (Bq/kg) of radionuclides (e.g., ^{238}U, ^{232}Th or

^{40}K); N_A is Avogadro's number (6,023x10^{23} atoms/mol); C is a unit conversion factor: 10^6 for uranium and thorium, or 10^2 for potassium. Accordingly, the elemental concentrations of uranium and thorium are expressed in parts per million (ppm), where 1 ppm equals 1 mg/kg, while potassium concentration is expressed as a percentage (%) due to its significantly higher natural abundance compared to uranium or thorium.

Alternatively, using standard conversion factors [24, 27-29]:

- 1 ppm U = 12.35 Bq/kg of ^{238}U;
- 1 ppm Th = 4.06 Bq/kg of ^{232}Th;
- 1% K = 313 Bq/kg of ^{40}K

Uncertainties on elemental concentrations were propagated from those on specific activities.

III. Results and Discussion

The specific activities of radionuclides from the ^{238}U and ^{232}Th decay series, as well as ^{40}K, were measured in the 30 soil samples collected on Nosy-Be Island. The detailed results, along with their statistical analysis, and their geo-pedological interpretation are presented below.

3.1. Specific Activities of Radionuclides and Statistical Analysis

The specific activities of the ^{238}U and ^{232}Th decay series and ^{40}K were quantified in the 30 soil samples. The measured values are reported in Table II.

The specific activity of the ^{238}U series ranges from 24 to 68 Bq/kg, with a mean of 33 ± 8 Bq/kg. For the ^{232}Th series values range from 22 to 71 Bq/kg, with an average of 39 ± 9 Bq/kg. The ^{40}K activity displays the greatest variability, ranging from 51 to 480 Bq/kg, with a mean value of 138 ± 79 Bq/kg.

Analysis of the statistical distributions (Table III) indicates that none of the three radionuclides follow a normal distribution, as confirmed by the Shapiro-Wilk test ($p < 0.05$).

Frequency histograms (Fig. 4, 5, and 6) and the high, positive skewness values (2.49 for ^{238}U, 1.44 for ^{232}Th, and 2.88 for ^{40}K) indicate right-skewed distributions. This shape suggests the presence of a few samples with significantly higher concentrations than the majority, interpreted as radiological hotspots. Sample NB24, with values of 68 Bq/kg (^{238}U), 71 Bq/kg (^{232}Th), and 480 Bq/kg (^{40}K), is identified as the main hotspot in this study.

When compared with global reference values published by UNSCEAR [1] (Table II), the results reflect the unique geochemical signature of Nosy-Be, assessed using both specific activities and elemental concentrations. For uranium, the mean specific activity of the ^{238}U series (33 ± 8 Bq/kg) and its corresponding elemental concentration (2.66 ± 0.69 ppm) are close to global averages of 35 Bq/kg and 2.83 ppm, respectively.

In contrast, thorium levels slightly exceed the global reference values. The mean specific activity of the ^{232}Th series is 39 ± 9 Bq/kg (versus the global average of 30 Bq/kg), and its corresponding concentration is 9.53 ± 2.25 ppm (compared to 7.39 ppm globally). This slight enrichment is consistent with the island's predominantly magmatic lithology, which naturally tends to be richer in thorium.

The most notable deviation involves potassium. The mean specific activity of ^{40}K, at 138 ± 79 Bq/kg, is significantly below the global average of 400 Bq/kg. Similarly, the mean elemental concentration of 0.44 ± 0.25 % is approximately one-third of the global average of 1.28 %. As shown in Table II, potassium values are highly variable, ranging from 51 Bq/kg to 480 Bq/kg, confirming considerable heterogeneity. This low concentration and high dispersion strongly indicate intense leaching, a phenomenon where the highly mobile potassium ions are readily washed away by heavy tropical rains. This leads to general depletion, especially in old and weathered soils.

Therefore, while uranium and thorium levels place Nosy-Be within a typical geochemical range for volcanic terrains, the marked potassium deficiency serves as a clear indicator of intense climatic weathering of the island's soils.

To further contextualize these results, the measured specific activities are compared to data from various regions of Madagascar, representing different geological settings (Table IV). This comparative analysis allows an assessment of Nosy-Be's radiological signature at the national scale and its placement relative to known high-radioactivity zones.

A marked contrast is observed with highly mineralized areas such as Ampasimbe (Fenoarivo Atsinanana district) and Fort-Dauphin, where radionuclide concentrations are several times higher than those in Nosy-Be [7, 30]. This confirms that Nosy-Be exhibits moderate natural radioactivity within the national context.

Comparisons with other Malagasy magmatic massifs reveal significant variations, even within similar geological contexts. For example, the Amber Mountain volcanic massif [3] has comparable ^{238}U activity (44 Bq/kg vs. 33 Bq/kg in Nosy-Be), but shows significantly higher levels of ^{232}Th (90 Bq/kg) and ^{40}K (218 Bq/kg).

TABLE II. Specific activities and elemental concentrations of natural radionuclides in the volcanic soil of Nosy-Be

Sample ID	GPS Coordination		Specific activity (Bq/kg)			Elemental concentration (ppm)		
	Latitude (N)	Longitude (E)	^{238}U	^{232}Th	^{40}K	U	Th	K
NB01	13°23'00.88"S	48°12'32.71"E	26 ± 2	30 ± 5	128 ± 6	2.11 ± 0.16	7.39 ± 1.23	0.41 ± 0.02
NB02	13°21'16.96"S	48°11'32.59"E	33 ± 2	41 ± 4	166 ± 6	2.67 ± 0.16	10.10 ± 0.99	0.53 ± 0.02
NB03	13°20'07.61"S	48°11'08.86"E	40 ± 2	46 ± 4	106 ± 5	3.24 ± 0.16	11.33 ± 0.99	0.34 ± 0.02
NB04	13°19'16.23"S	48°13'49.09"E	27 ± 2	47 ± 4	122 ± 6	2.19 ± 0.16	11.58 ± 0.99	0.39 ± 0.02
NB05	13°17'41.38"S	48°11'58.99"E	41 ± 3	44 ± 8	175 ± 11	3.32 ± 0.24	10.84 ± 1.97	0.56 ± 0.04
NB06	13°16'03.83"S	48°11'46.68"E	31 ± 2	34 ± 5	178 ± 7	2.51 ± 0.16	8.37 ± 1.23	0.57 ± 0.02
NB07	13°17'10.87"S	48°15'09.06"E	33 ± 2	34 ± 4	134 ± 6	2.67 ± 0.16	8.37 ± 0.99	0.43 ± 0.02
NB08	13°13'40.58"S	48°15'22.59"E	39 ± 2	39 ± 4	51 ± 4	3.16 ± 0.16	9.61 ± 0.99	0.16 ± 0.01
NB09	13°13'07.20"S	48°16'43.08"E	34 ± 1	32 ± 3	194 ± 6	2.75 ± 0.08	7.88 ± 0.74	0.62 ± 0.02
NB10	13°14'07.47"S	48°18'08.84"E	35 ± 1	44 ± 3	146 ± 5	2.83 ± 0.08	10.84 ± 0.74	0.47 ± 0.02
NB11	13°16'35.65"S	48°19'29.49"E	33 ± 2	30 ± 5	138 ± 6	2.67 ± 0.16	7.39 ± 1.23	0.44 ± 0.02

NB12	13°19'13.56"S	48°16'45.28"E	26 ± 1	36 ± 3	52 ± 3	2.11 ± 0.08	8.87 ± 0.74	0.17 ± 0.01
NB13	13°19'39.27"S	48°19'44.28"E	43 ± 1	51 ± 4	214 ± 7	3.48 ± 0.08	12.56 ± 0.99	0.68 ± 0.02
NB14	13°22'02.59"S	48°18'59.23"E	42 ± 2	40 ± 4	128 ± 6	3.40 ± 0.16	9.85 ± 0.99	0.41 ± 0.02
NB15	13°23'22.44"S	48°20'29.59"E	34 ± 2	37 ± 4	157 ± 6	2.75 ± 0.16	9.11 ± 0.99	0.50 ± 0.02
NB16	13°24'34.38"S	48°21'19.77"E	24 ± 1	22 ± 3	73 ± 3	1.94 ± 0.08	5.42 ± 0.74	0.23 ± 0.01
NB17	13°24'03.86"S	48°18'07.53"E	32 ± 2	42 ± 4	64 ± 4	2.59 ± 0.16	10.34 ± 0.99	0.20 ± 0.01
NB18	13°23'24.64"S	48°16'22.27"E	29 ± 2	38 ± 5	100 ± 6	2.35 ± 0.16	9.36 ± 1.23	0.32 ± 0.02
NB19	13°24'24.96"S	48°16'30.32"E	35 ± 2	37 ± 5	130 ± 7	2.83 ± 0.16	9.11 ± 1.23	0.42 ± 0.02
NB20	13°24'20.26"S	48°15'19.17"E	27 ± 2	34 ± 6	185 ± 8	2.19 ± 0.16	8.37 ± 1.48	0.59 ± 0.03
NB21	13°24'03.93"S	48°14'38.67"E	33 ± 2	44 ± 5	129 ± 6	2.67 ± 0.16	10.84 ± 1.23	0.41 ± 0.02
NB22	13°23'08.44"S	48°14'53.07"E	25 ± 2	36 ± 5	138 ± 7	2.02 ± 0.16	8.87 ± 1.23	0.44 ± 0.02
NB23	13°23'25.90"S	48°15'28.80"E	32 ± 2	33 ± 5	109 ± 6	2.59 ± 0.16	8.13 ± 1.23	0.35 ± 0.02
NB24	13°21'24.89"S	48°15'25.07"E	68 ± 3	71 ± 7	480 ± 16	5.51 ± 0.24	17.49 ± 1.72	1.53 ± 0.05
NB25	13°26'31.79"S	48°20'49.39"E	25 ± 1	27 ± 3	68 ± 4	2.02 ± 0.08	6.65 ± 0.74	0.22 ± 0.01
NB26	13°27'01.76"S	48°21'35.57"E	24 ± 1	30 ± 3	92± 4	1.94 ± 0.08	7.39 ± 0.74	0.29 ± 0.01
NB27	13°28'38.74"S	48°22'16.80"E	28 ± 1	35 ± 3	104 ± 5	2.27 ± 0.08	8.62 ± 0.74	0.33 ± 0.02
NB28	13°29'41.33"S	48°21'33.92"E	28 ± 2	51 ± 4	99 ± 5	2.27 ± 0.16	12.56 ± 0.99	0.32 ± 0.02
NB29	13°29'48.19"S	48°20'29.75"E	32 ± 2	42 ± 4	64 ± 4	2.59 ± 0.16	10.34 ± 0.99	0.20 ± 0.01
NB30	13°27'25.09"S	48°19'32.92"E	28 ± 2	34 ± 5	205 ± 8	2.27 ± 0.16	8.37 ± 1.23	0.65 ± 0.03
Mean ± Standard Deviation			33 ± 8	39 ± 9	138 ± 79	2.66 ± 0.69	9.53 ± 2.25	0.44 ± 0.25
(Minimal value – maximal value)			(24 – 68)	(22 – 71)	(51 – 480)	(1.94 – 5.51)	(5.42 – 17.49)	(0.16 – 1.53)
Worldwide mean value*			35	30	400	2.83	7.39	1.28

* These average values were obtained by converting the worldwide average activity concentrations for ^{232}Th (30 Bq/kg), ^{238}U (35 Bq/kg), and ^{40}K (400 Bq/kg), as reported in the UNSCEAR 2000 report [1], into their respective elemental concentrations using Equation (14).

To contextualize the present results, the specific activities measured in the soils of Nosy-Be are also compared to literature data from different regions of Madagascar, which represent various geological contexts (Table IV). This comparative analysis allows for an evaluation of Nosy-Be's radiological signature on a national scale and to position it relative to regions known for their high radioactivity levels.

The analysis reveals a striking contrast with high-mineralization zones such as Ampasimbe (district of Fenoarivo Atsinanana) and Fort-Dauphin. The mean specific activities of the three natural radionuclides in the soils of Nosy-Be are several orders of magnitude lower than those in these two localities [7, 30]. This confirms that, within Madagascar, Nosy-Be is a region of moderate natural radioactivity.

Comparison with other Malagasy magmatic massifs reveals notable variations despite sometimes similar geological contexts. The Amber Mountain volcanic massif [3], for example, exhibits comparable activity levels for ^{238}U (44 Bq/kg vs. 33 Bq/kg in Nosy-Be), but markedly higher levels for ^{232}Th (90 Bq/kg) and ^{40}K (218 Bq/kg).

TABLE III. Statistical distribution of the activities of natural radionuclides

Statistical parameters	^{238}U	^{232}Th	^{40}K
Number of samples	30	30	30
Mode	33.00	34.00	64.00[a]
Mean	32.90	38.70	137.63
Std. Error of Mean	1.56	1.67	14.40
Std. Deviation	8.56	9.14	78.90
Minimum	24.00	22.00	51.00
25th percentile	27.00	33.75	97.25
50th percentile (Median)	32.00	37.00	128.50
75th percentile	35.00	44.00	168.25
Maximum	68.00	71.00	480.00
Skewness	2.49	1.44	2.88
Kurtosis	9.11	4.33	12.03
Test of Normality (Shapiro-Wilk)	<0.001	0.011	<0.001

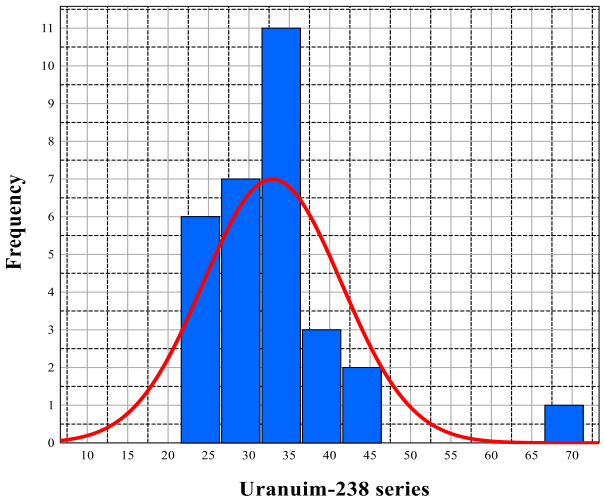

Fig. 4. Frequency distribution of specific activities of the ^{238}U series

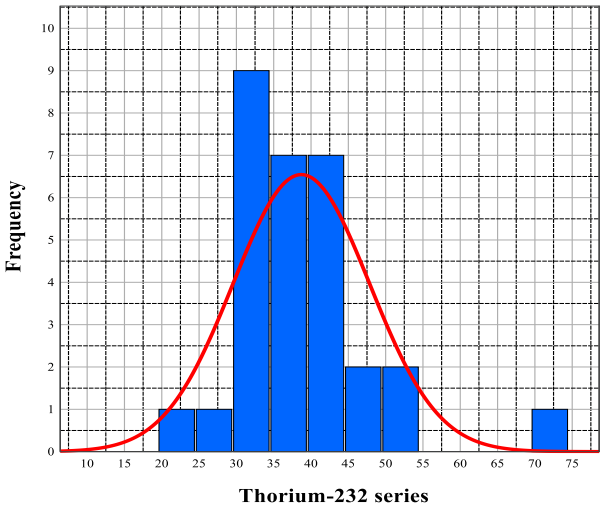

Fig. 5. Frequency distribution of specific activities of the ^{232}Th series

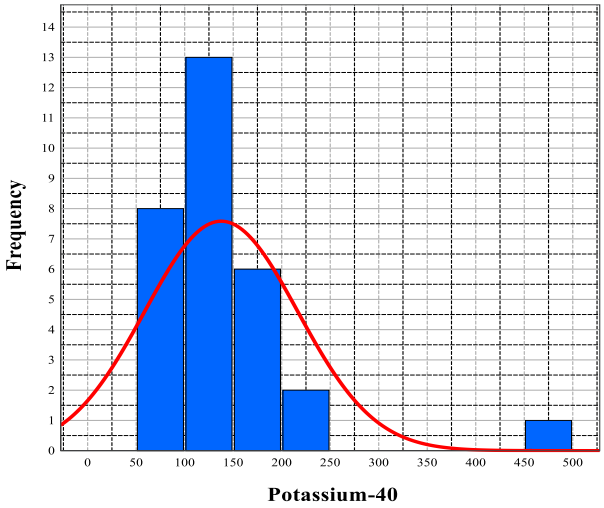

Fig. 6. Frequency distribution of specific activities of ^{40}K

The Vakinankaratra region [31], which encompasses the Ankaratra volcanic complex, exhibits considerably higher concentrations for all three radionuclides (176 Bq/kg for ^{238}U, 126 Bq/kg for ^{232}Th, and 467 Bq/kg for ^{40}K), reflecting a much richer geochemical signature. In contrast, the Ambilobe district [22], also of volcanic origin, presents lower levels of ^{238}U (18 Bq/kg), similar ^{232}Th activity (40 Bq/kg), and notably higher ^{40}K content (518 Bq/kg). These findings demonstrate that, even in volcanic settings, radionuclide distribution is governed by the unique geochemistry of each magmatic province.

An analysis of nearby regions with distinct geochemical traits is also illuminating. Although part of the same northwestern magmatic province, Nosy-Be differs significantly from adjacent areas that have undergone elemental enrichment. The Ampasindava peninsula [32], which hosts a rare earth element (REE) deposit, is notably enriched in ^{238}U (76 Bq/kg) and especially in ^{232}Th (261 Bq/kg), consistent with REE-associated radioactivity. Similarly, Ambanja and its surroundings [18], known for alkaline rocks and carbonatite intrusions, exhibit elevated activity levels, particularly for ^{232}Th (123 Bq/kg) and ^{40}K (730 Bq/kg). These comparisons demonstrate that Nosy-Be has not experienced the same radiogenic enrichment processes as its neighbours.

Finally, comparisons with non-volcanic settings offer further insights. In crystalline basement regions, Nosy-Be soils are geochemically distinct. Areas such as Antananarivo [7] and Befandriana Nord [33], both underlain by Precambrian basement and lateritic soils, show lower ^{238}U levels (14 and 21 Bq/kg, respectively) but much higher activities for ^{232}Th (75 and 198 Bq/kg) and ^{40}K (448 and 200 Bq/kg), reflecting granitic and metamorphic influences.

In contrast, Nosy-Be shares similarities with sedimentary and coastal formations that lack concentrated mineralization. This is the case in the Antalaha district (33 Bq/kg for ^{238}U, 54 Bq/kg for ^{232}Th) [10], and the Antalaha-Ambohitralanana coastline, which shows nearly identical values (34 Bq/kg for ^{238}U and 38 Bq/kg for ^{232}Th) [5]. However, this context differs sharply from the coastal sands of the Antsiranana I region, where sedimentary sorting processes have led to high ^{238}U levels (109 to 139 Bq/kg in Ramena, Orangea, and Baie des Français beach sands) [20, 34], a phenomenon absent in Nosy-Be's volcanic soils.

In summary, this comprehensive comparative analysis confirms that the soils of Nosy-Be exhibit moderate natural radioactivity. Their radiological signature is distinct from that of other volcanic centers, lacks the enrichment observed in neighboring regions, and differs fundamentally from that of crystalline basement or mineral-rich coastal sands. These findings highlight the primary role of parent rock lithology and local weathering processes in governing radionuclide distribution in soils.

TABLE IV. Comparison of similar study of natural radioactivity in soil samples from different localities of Madagascar

Locality	Average specific activity (Bq/kg)			Reference
	^{238}U	^{232}Th	^{40}K	
Nosy-Be	33	39	138	Present work
Amber Mountain, Antsiranana II	44	90	218	[3]
Antalaha-Ambohitralanana littoral zone	34	38	300	[5]
Antananarivo	14	75	448	[7]
Fort-Dauphin	299	1827	420	[7]
Antalaha District	33	54	277	[9]
Ambanja city and its Surroundings	44	123	730	[17]
Ramena-Orangea beach, Antsiranana II	109	77	198	[19]
Ambilobe District	18	40	518	[21]
Ampasimbe, Fenoarivo Atsinanana District	5390	21336	575	[29]
Vakinankaratra, Antsirabe	176	126	467	[30]
Ampasindava peninsula, Ambanja	76	261	355	[31]
Befandriana Nord District	21	198	200	[32]
Baie des Français littoral zone, Antsiranana I	139	126	313	[33]

3.2. Spatial Distribution Analysis and Geo-pedological Correlation

The spatial distribution of radionuclides on Nosy-Be reveals a coherent pattern, primarily controlled by the dual influence of the island's geological substrate and the intensity of weathering processes. This interpretation is further supported by comparisons with European geochemical baselines and analogous volcanic settings.

Fig. 7 illustrates the spatial distribution of ^{238}U. The highest specific activities (ranging from 44 to 68 Bq/kg), corresponding to uranium concentrations of up to 5.51 ppm, are consistently located in the western part of the island. This sector is characterized by relatively recent (Pleistocene) volcanic formations composed of rhyolites and basalts. Uranium, being an incompatible element, tends to concentrate in these differentiated magmatic rocks during crystallization. The youthful soils derived from these rocks, having undergone limited weathering, have largely preserved this primary geochemical signature. In contrast, the eastern part of the island, dominated by older and intensely weathered ferrallitic soils, exhibits lower and more homogeneous uranium levels (typically between 24 and 35 Bq/kg).

International Journal of Scientific Engineering and Science
Volume 9, Issue 7, pp. 36-45, 2025. ISSN (Online): 2456-7361

The mean uranium concentration in Nosy-Be soils (2.66 ppm) is close to the median value reported for European surface soils (2.94 ppm) [8]. Even the island's hotspot (5.51 ppm) remains moderate in comparison to other active volcanic regions, such as the Aeolian Islands, where uranium concentrations in recent rhyolitic rocks can reach up to 20.0 ppm [19]. This confirms that uranium-related radioactivity in Nosy-Be, although spatially heterogeneous, falls within a moderate and geochemically normal range.

In comparison, the mean uranium concentration in Nosy-Be soils (2.66 ppm) is very close to the median estimated for European surface soils, which is 2.94 ppm [8]. Even the hotspot of Nosy-Be (5.51 ppm) remains a moderate value, well below the concentrations observed in other active volcanic contexts such as the Aeolian Islands, where recent rhyolitic rocks can reach 20.0 ppm of uranium [19]. This confirms that the uranium radioactivity of Nosy-Be, although heterogeneous, is within a moderate range.

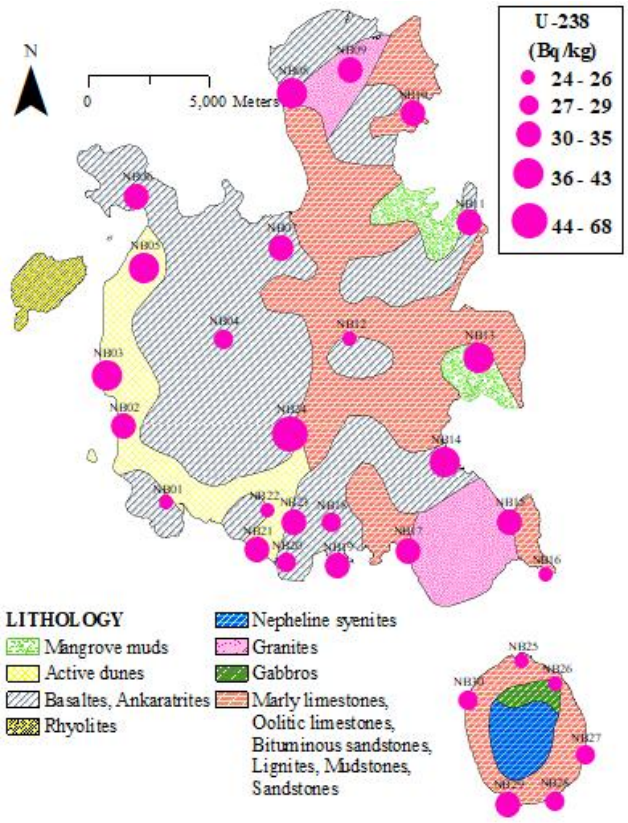

Fig. 7. Influence of geological formations on the specific activity of the ^{238}U series in the volcanic soil of Nosy-Be

A similar distribution pattern is observed for ^{232}Th, as shown in Fig. 8. The highest specific activities (52 to 71 Bq/kg), corresponding to concentrations up to 17.49 ppm, are also found in the island's western sector, closely associated with the same volcanic formations. Consistent with its geochemical behavior, thorium was co-enriched with uranium in these magmatic rocks. However, the east–west gradient in thorium distribution is less pronounced than for potassium. This is attributable to thorium's extremely low geochemical mobility, which enables it to remain relatively immobile even in highly weathered profiles. As a result, thorium is better conserved in situ, even in the older and more altered soils of the eastern part of the island.

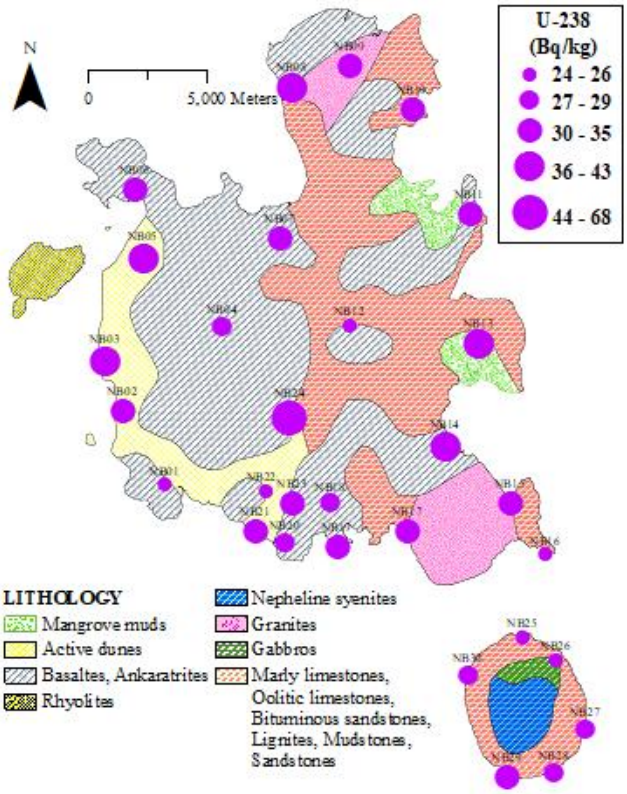

Fig. 8. Influence of geological formations on the specific activity of the ^{232}Th series in the volcanic soil of Nosy-Be

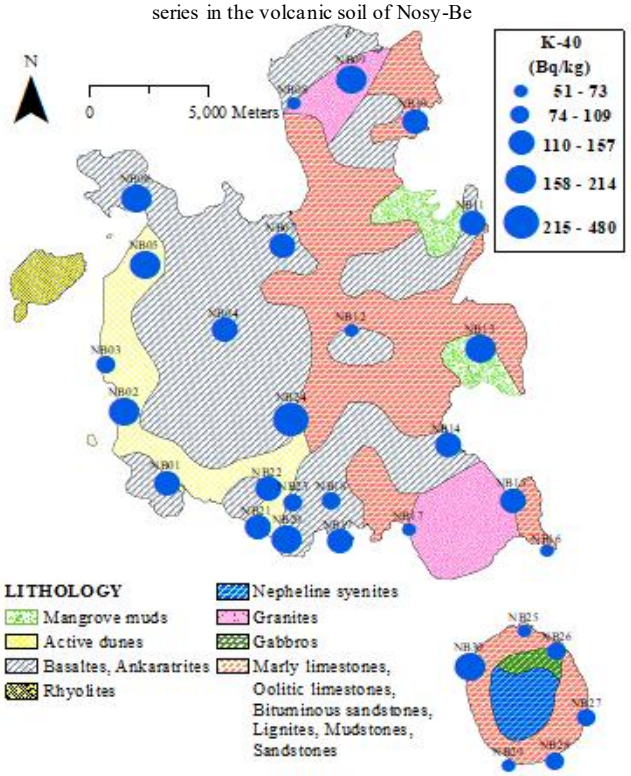

Fig. 9. Influence of geological formations on the specific activity of the ^{40}K in the volcanic **soil** of Nosy-Be

The mean thorium concentration in Nosy-Be (9.53 ppm) is almost identical to the European soil median (9.3 ppm) [8], reinforcing the characterization of the island as geochemically standard in terms of thorium content. Again, comparison with the Aeolian Islands highlights Nosy-Be's moderate nature: felsic formations on Vulcano Island can exhibit thorium concentrations as high as 63.4 ppm [19], nearly four times the island's maximum value. Thus, thorium distribution supports the geological interpretation while confirming the absence of anomalous radioactivity.

In contrast, the most striking geo-radiological disparity concerns ^{40}K, as depicted in Fig. 9. The highest specific activities (ranging from 215 to 480 Bq/kg), corresponding to potassium concentrations between 0.68% and 1.53%, are strongly concentrated in the western region. These elevated values reflect the abundance of potassium-bearing minerals (notably feldspars) in the young volcanic rocks. Conversely, the eastern and central parts of the island exhibit marked depletion, with specific activities frequently below 100 Bq/kg (i.e., potassium concentrations below 0.32%). This profound deficit clearly illustrates the effects of long-term, intense leaching processes under tropical climatic conditions, which lead to substantial loss of this highly mobile element.

Potassium depletion is arguably the most distinctive geochemical feature of Nosy-Be on a continental scale. The island's average potassium concentration (0.44%) is far below the European median of approximately 1.58% [8]. Even its highest recorded value (1.53%) barely reaches the European mean. When compared to potassium-rich Italian volcanic rocks, which can reach concentrations of up to 6.1% [19], the relative scarcity of potassium in Nosy-Be becomes even more evident. These findings clearly demonstrate that potassium distribution is the most sensitive tracer of both parent rock composition and the intensity of climatic weathering on the island.

Overall, a pronounced geo-radiological contrast emerges between the younger, radiologically enriched western part of Nosy-Be and its older, heavily weathered and radiologically depleted eastern sector, especially with respect to potassium. Intense chemical weathering, amplified by tropical rainfall and erosion, acts as the principal driver of elemental redistribution, ultimately controlling the observed spatial heterogeneity in natural radioactivity across the island's surface.

IV. Conclusion

This study presents the first comprehensive assessment of natural radioactivity and spatial distribution mapping of ^{238}U, ^{232}Th, and ^{40}K in the volcanic soils of Nosy-Be Island. The measured mean specific activities 33 ± 8 Bq/kg for the ^{238}U series, 39 ± 9 Bq/kg for the ^{232}Th series, and 138 ± 79 Bq/kg for ^{40}K position Nosy-Be as a region of moderate natural radioactivity, both at the national level and in comparison, with international reference values. Unlike other geological zones in Madagascar, the island does not exhibit extreme radiological anomalies.

The principal contribution of this work lies in the demonstration of marked spatial heterogeneity, driven by the dual influence of geology and pedology, thus confirming the central hypothesis of the study. A clear contrast emerges between the eastern part of the island, dominated by ancient, highly weathered, and leached ferrallitic soils with significantly depleted ^{40}K content, and the western part, characterized by recent volcanic formations and immature soils. The latter retains elevated concentrations of radionuclides, particularly potassium and includes the radiological hotspots identified in this survey.

This work establishes the first radiological baseline map of Nosy-Be, a critical tool for future environmental monitoring, regional geochemical studies, and the sustainable management of natural resources. It provides a scientific foundation for further multidisciplinary investigations.

It is important to emphasize that this study focuses solely on the geochemical characterization and quantification of natural radionuclide concentrations. It does not assess their potential health impacts. Consequently, these results constitute essential baseline data for future radiological risk assessments, particularly for modeling and quantifying external dose rates affecting both the local population and visitors.

Acknowledgment

The authors would like to express their sincere gratitude to the Nuclear Techniques and Analysis at INSTN-Madagascar and Nuclear Metrology and Environment at the University of Antsiranana for their invaluable technical support and collaboration throughout the course of this research.

References

[1] UNSCEAR. Sources and effects of ionizing radiation, Vol. 1. United Nations Scientific Committee on the Effects of Atomic Radiation. Report of the General Assembly with Scientific Annexes. United Nations, New York; 2000.

[2] M. Tzortzis, H. Tsertos, S. Christofides, G. Christodoulides. Gamma-ray measurements of naturally occurring radioactive samples from Cyprus characteristic geological rocks. *Radiation Measurements*, Vol. 37, Issue 3, pp. 221-229, 2003. https://doi.org/10.1016/S1350-4487(03)00028-3.

[3] Z. Donné, M. Rasolonirina, H.C. Djaovagnono, B. Kall, N. Rabesiranana & J. Rajaobelison. Study of water radioactivity transfer from telluric origin in the Amber Mountain, Antsiranana, Madagascar. *Scientific African*; 13 (2021): e00902.

[4] N. M. Demewoz, L. N. Kassie, H. G. Zeleke. Assessment of radioactivity in soil samples from Wolaita Sodo town, Ethiopia: implications for environmental and public health. *Radiation Protection Dosimetry;* Vol. 201, Issue 3; pp. 160–177, 2025. https://doi.org/10.1093/rpd/ncaf002

[5] A.F. Barijaona, F. Asimanana & M. Rasolonirina. Contribution à l'étude de la radioactivité naturelle, par spectrométrie gamma, du sol dans la zone littorale d'Antalaha-Ambohitralanana Madagascar. *Afrique Science*, Vol. 13, No. 2, 2017.

[6] N. H. Apriantoro, A. T. Ramli, S. Sutisna, Activity Concentration of 238U, 232Th and 40K Based on Soil Types in Perak State, Malaysia. *Earth Science Research*; Vol. 2, No. 2; pp. 122-127; 2013, https://doi.org/10.5539/esr.v2n2p122

[7] N. Rabesiranana. Contribution à l'étude de la radioactivité environnementale à Madagascar : de la quantification à l'utilisation des traceurs radio-isotopiques environnementaux. *HDR, Université d'Antananarivo, Madagascar*, pp. 1-140, 2017. http://biblio.univ-antananarivo.mg/pdfs/rabesirananaNaivo1_PC_HDR_17.pdf

[8] European Commission, Joint Research Centre. Terrestrial radionuclides. In T. Tollefsen, G. Cinelli, T. A. De Meijer, P. Bossew, & M. De Cort (Eds.), European Atlas of Natural Radiation, *Publication Office of the European Union, Luxembourg*; pp. 58–87, 2019. https://data.europa.eu/doi/10.2760/46388

[9] S. K. Anguma, V. Habakwiha & I. Habumugisha. Determination of natural radioactivity and hazards in volcanic soils of Kisoro district in south-western Uganda. *Kabale University Interdisciplinary Research*

Journal (KURJ); Vol. 2, Issue 2; pp. 193-203; 2023.

[10] F. Ngoko, A. F. Solonjara, Z. Donné, D. Rasolozafy, and B. Kall. Étude de la radioactivité naturelle du sol : Cas du district d'Antalaha, région de SAVA, nord-est de Madagascar. *American Journal of Innovative Research and Applied Sciences*. Vol. 19, No 4, pp. 27-38, 2024. Doi: https://doi.org/10.5281/zenodo.13844565

[11] M. López-Pérez, C. Martín-Luis, F. Hernández, E. Liger, J. C. Fernández-Aldecoa, J. M. Lorenzo-Salazar, J. Hernández-Armas, P. A. Salazar-Carballo. Natural and artificial gamma-emitting radionuclides in volcanic soils of the Western Canary Islands, *Journal of Geochemical Exploration*, Vol. 229, 2021. https://doi.org/10.1016/j.gexplo.2021.106840.

[12] J. Vieillefon & F. Bourgeat. Notice explicative - Cartes pédologiques de reconnaissance au 1/50.000 - Feuille de Nosy-Be. *ORSTOM (aujourd'hui IRD), Antananarivo*. 1964.

[13] L. Melluso & V. Morra. Petrogenesis of Late Cenozoic mafic alkaline rocks of the Nosy Be archipelago (northern Madagascar): relationships with the Comorean magmatism *Journal of Volcanology and Geothermal Research*, Vol. 96, Issue. 1-2, pp. 129-150, 2000. https://doi.org/10.1016/S0377-0273(99)00139-0.

[14] S. Mbotimary. Typologie du tourisme et activités touristiques dans le Parc National Marin Nosy Tanikely (Nosy-Be, Nord-Ouest de Madagascar). Mémoire de Licence. *Faculté des Sciences de Technologies et de l'Environnement, Université de Mahajanga* ; pp. 1-41, 2015.

[15] P. Chiozzi, P. De Felice, V. Pasquale, D. Russo, M. Verdoya. Field γ-ray spectrometry on the Vulcano island (Aeolian Arc, Italy), Applied Radiation and Isotopes, Vol. 51, Issue 2, pp. 247-253, 1999. https://doi.org/10.1016/S0969-8043(98)00181-X.

[16] I. Rosianna, E. D. Nugraha, H. Syaeful, S. Putra, M. Hosoda, N. Akata, & S. Tokonami. Natural Radioactivity of Laterite and Volcanic Rock Sample for Radioactive Mineral Exploration in Mamuju, Indonesia. *Geosciences*, Vol. 10, Issue 9, pp. 1-13, 2020. https://doi.org/10.3390/geosciences10090376

[17] R. Marques, M. I. Prudêncio, D. Russo, G. Cardoso, M. I. Dias, A. L. Rodrigues, M. Reis, M. Santos & F. Rocha. Evaluation of naturally occurring radionuclides (K, Th and U) in volcanic soils from Fogo Island, Cape Verde. *Journal of Radioanalytical and Nuclear Chemistry*; Vol. 330, Issue 1; pp. 347–355; 2021. https://doi.org/10.1007/s10967-021-07959-7

[18] J. E. Rahelivao, Z. Donné, A. Razafindrapata, A. I. Joelisoafara, M. Rasolonirina & B. Kall. Study of Natural Radioactivity Levels and the Associated Radiological Hazards in Soil from Ambanja City and its Surroundings, Madagascar. *International Journal of Innovative Research in Science, Engineering and Technology*. Vol. 12, Issue 5, 2023. DOI:10.15680/IJIRSET.2023.1202005

[19] P. Chiozzi, P. De Felice, A. Fazio, V. Pasquale, M. Verdoya. Laboratory application of NaI(Tl) γ-ray spectrometry to studies of natural radioactivity in geophysics, Applied Radiation and Isotopes, Vol. 53, Issues 1–2, pp. 127-132, 2000. https://doi.org/10.1016/S0969-8043(00)00123-8.

[20] B. Kall, Z. Donné, M. Rasolonirina, N. Rabesiranana & G. Rambolamanana. Contribution à l'étude de la radioactivité gamma du sable des plages de Ramena et d'Orangea, Antsiranana, Madagascar. *Afrique Science*. Vol. 10, No. 4, pp. 23- 35, 2014.

[21] G. Cinelli, L. Tositti, D. Mostacci, J. Baré. Calibration with MCNP of NaI detector for the determination of natural radioactivity levels in the field. Journal of Environmental Radioactivity; Vol. 155–156, pp. 31-37, 2016, https://doi.org/10.1016/j.jenvrad.2016.02.009.

[22] J. P. Stolerie, M. Rasolonirina, Z. Donné, B. Kall & N. Rabesiranana. Etude de la radioactivité naturelle d'origine tellurique du district d'Ambilobe, Madagascar. *American Journal of Innovative Research Applied Sciences*. Vol. 13, No. 5, pp. 518-529, 2021.

[23] P. Chiozzi, V. Pasquale, M. Verdoya, S. Minato. Natural gamma-radiation in the Aeolian volcanic arc, Applied Radiation and Isotopes, Vol. 55, Issue 5, pp. 737-744, 2001. https://doi.org/10.1016/S0969-8043(01)00127-0.

[24] S. S. Kaintura, S. Devi, K. Tiwari, S. Thakur, R. Sebastian & P. P. Singh, Gamma-spectroscopic assessment of radionuclides and radiological hazards in undisturbed and cultivated soils of Rupnagar, Punjab, India. Nuclear Engineering and Technology, Vol 57, Issue 6, 103418, ISSN 1738-5733, 2025. https://doi.org/10.1016/j.net.2024.103418

[25] M. Tzortzis, & H. Tsertos. Determination of Thorium, Uranium and Potassium Elemental Concentrations in Surface Soils in Cyprus. *Journal of Environmental Radioactivity*, Vol. 77, pp. 325-338, 2004. https://doi.org/10.1016/j.jenvrad.2004.03.014

[26] S. T. Gbenu, S. F. Olukotun, O. F. Oladejo, C. A. Onumejor, F. O. Balogun, F. I. Ibitoye, M. K. Fasasi. Assessment of the Elemental Concentration of Potassium, Uranium and Thorium with their Associated Radiogenic Heat Production in Granite Rocks of Southwestern Nigeria. Journal of Radiation and Nuclear Applications, Vol. 5, No. 3, pp. 205-210, 2020. http://dx.doi.org/10.18576/jrna/050307

[27] A.D. Bajoga, A.N. Al-Dabbous, A.S. Abdullahi, N.A. Alazemi, Y.D. Bachama, S.O. Alaswad, Evaluation of elemental concentrations of uranium, thorium and potassium in top soils from Kuwait. *Nuclear Engineering and Technology*, Vol. 51, Issue 6, pp. 1638-1649, 2019. https://doi.org/10.1016/j.net.2019.04.021

[28] P. Shaba, K. K. Maseka, and P. Hayumbu. Evaluation of Radiological Risk Hazards in Sediments and Selected Streams Around Kalulushi and Kitwe Towns. *Archives of Microbiology and Immunology*, Vol. 8, Issue 4, pp. 472-479, 2024. DOI: 10.26502/ami.936500194

[29] G. Erdi-Krausz, M. Matolin, B. Minty, J. P. Nicolet, W. S. Reford & E. M. Schetselaar. *Guidelines for radioelement mapping using gamma ray spectrometry data: also, as open access e-book*. (IAEA-TECDOC; Vol. 1363). International Atomic Energy Agency (IAEA), 2003. http://www-pub.iaea.org/MTCD/publications/PDF/te_1363_web.pdf

[30] T. H. Randriamora, H. A. Razafindramiandra, Raoelina Andriambololona, S. D. Ravelomanantsoa, M. A. L. Ralaivelo, M. Rasolonirina, J. L. R. Zafimanjato, H. F. Randriantseheno. Determination of Natural Radioactivity in the North East Beach Sands of Madagascar. *American Journal of Physics and Applications*, Vol. 5, Issue 1, 6-12, 2017. https://doi.org/10.11648/j.ajpa.20170501.12

[31] H. A. Razafindramiandra. Radioprotection du public suite aux études comparatives de la dose efficace annuelle reçue entre la méthode directe et indirecte, Cas de la zone uranifère de Vinaninkarena, Antsirabe. Thèse de Doctorat en Physique Nucléaire Appliquée et Physique des Hautes Energies de l'Université d'Antananarivo Madagascar (2017).

[32] O. Rafidimanantsoa, M. Rasolonirina, Z. Donné, P. H. Ralaiarison, S. Tonissa, N. Rabesiranana & R. J. L. Zafimanjato. Caractérisation de la radioactivité naturelle du gisement des terres rares, de la presqu'île d'Ampasindava du nord-ouest de Madagascar. *American Journal of Innovative Research Applied Sciences*. Vol 13, No. 4, pp. 452-461, 2021.

[33] A. Randrianarivo, F. Asivelo Solonjara & F. Asimanana. Contribution à l'étude de la radioactivité du sol de district de Befandriana-Nord, Madagascar. *American Journal of Innovative Research and Applied Sciences*. Vol. 4, No. 1, pp. 22-28, 2017.

[34] B. Kall, T. Tombo, M. Rasolonirina, N. Rabesiranana & G. Rambolamanana. Contribution à l'étude de dose due à la radioactivité gamma du sol sur la rive de la baie des Français, Antsiranana, Madagascar. *Afrique Science*, ISSN 1813-548X, Vol. 11, No. 1, pp. 122-135, 2015.